

## Research article

# Effects of Moleac 901 after severe spinal cord injury on chronic phase in Wistar rats

Dewa Putu Wisnu Wardhana<sup>a,\*</sup>, Sri Maliawan<sup>b</sup>, Tjokorda Gde Bagus Mahadewa<sup>b</sup>, Andi Asadul Islam<sup>c</sup>, I Made Jawi<sup>d</sup>, Anak Agung Wiradewi Lestari<sup>e</sup>, I Gusti Kamasan Nyoman Arijana<sup>f</sup>, Rohadi Muhammad Rosyidi<sup>g</sup>, Sinta Wiranata<sup>h</sup>

<sup>a</sup> Neurosurgery Division, Department of Surgery, Faculty of Medicine, Universitas Udayana, Udayana University Hospital, 80361, Badung, Indonesia

<sup>b</sup> Neurosurgery Division, Department of Surgery, Faculty of Medicine, Universitas Udayana, Dr. IGNG Ngoerah General Hospital, 80113, Denpasar, Indonesia

<sup>c</sup> Department of Neurosurgery, Faculty of Medicine, Universitas Hasanuddin, 90245, Makassar, Indonesia

<sup>d</sup> Department of Pharmacology and Therapy, Faculty of Medicine, Universitas Udayana, 80232, Denpasar, Indonesia

<sup>e</sup> Department of Clinical Pathology, Faculty of Medicine, Universitas Udayana, Dr. IGNG Ngoerah General Hospital, 80113, Denpasar, Indonesia

<sup>f</sup> Departement of Histology, Faculty of Medicine, Universitas Udayana, 80232, Denpasar, Indonesia

<sup>g</sup> Department of Neurosurgery, Medical Faculty of Mataram University, West Nusa Tenggara General Hospital, 84371, Mataram, Indonesia

<sup>h</sup> Faculty of Medicine, Universitas Udayana, 80232, Denpasar, Indonesia

## ARTICLE INFO

## Keywords:

MLC901  
Spinal cord injury  
Caspase-3  
IL-10  
NG2

## ABSTRACT

**Background:** MLC901 is a phytopharmaceutical comprising significant compounds that can induce microenvironments conducive to the proliferation and specialization of neural cell progenitors. This study investigates the impact of administering MLC901, reducing the expression of NG2 and caspase-3 and increasing IL-10 levels, as well as histopathological and motor function, after severe spinal cord injury (SCI) in the chronic phase.

**Methods:** The study employed a randomized post-test-only control group design conducted between February and April 2023 at the Integrated Biomedical Laboratory. The participants in this study were categorized into three distinct groups: normal control, negative control, and therapy. A cohort of 18 rats was utilized for the study, with each group assigned a random allocation of six rats as subjects.

**Results:** The findings demonstrated a statistically significant disparity in the average NG2 expression ( $-52.00 \pm 20.03$ ;  $p \leq 0.05$ ), as well as Caspase-3 expression ( $-94.89 \pm 8.57$ ;  $p \leq 0.05$ ), which exhibited a lower magnitude. The levels of IL-10 ( $8.96 \pm 3.98$ ;  $p \leq 0.05$ ) were observed to be higher, along with an elevation in BBB score ( $7.67 \pm 0.89$ ;  $p \leq 0.05$ ), which was more pronounced in the treatment group compared to the negative control group. The cut-off point for cavitation diameter is determined to be  $114.915 \mu\text{m}$ , exhibiting a sensitivity and specificity of 100%. The area under curve (AUC) value is 1.0. The administration of MLC901 demonstrated a strong positive correlation with the increase in IL-10 levels ( $B 8.968$ ;  $p \leq 0.05$ ), as well as a substantial negative correlation with the decrease in Caspase-3 expression ( $B -52.000$ ;  $p \leq 0.05$ ) and NG2 expression ( $B -94.892$ ;  $p \leq 0.05$ ). The administration of MLC901 via the upregulation of NG2 and Caspase-3 significantly increased the Basso, Beattie, and Bresnahan (BBB) scores.

\* Corresponding author.

E-mail address: [wisnu\\_wardhana@unud.ac.id](mailto:wisnu_wardhana@unud.ac.id) (D.P. Wisnu Wardhana).

*Conclusions:* MLC901 positively affects motor and histopathological outcomes in the chronic phase of severe SCI in the Wistar rat model. These benefits are believed to be achieved by suppressing gliosis, neuroapoptosis, and neuroinflammation processes.

## 1. Introduction

Central nervous system (CNS) injuries are categorized into two types based on their location: brain injuries and spinal cord injuries. Spinal cord injury (SCI) is an abrupt neurological condition that leads to mortality or impairment in motor, sensory, and autonomic functioning [1,2]. The number of SCI patients is estimated at three million worldwide. The annual incidence rate of SCI is around 12,000 new cases. The mortality rate attributed to SCI in developing nations ranges from 1.4% to 20%. Mortality resulting from SCI is more prevalent in individuals aged 60 years and above. When considering the length of time, the disease lasts, fatality is most frequently observed within one year from the onset of SCI. This injury often results in a total impairment and impacts the cervical region [3].

The pathophysiological mechanism of SCI involves initial mechanical damage and compression of the spinal cord, which then triggers a series of biochemical and cellular processes called secondary injury [4]. This phase is marked by a sequential series of events, which include tissue swelling, oxidative stress, inflammation, nerve damage caused by excessive glutamate activity, generation of harmful free radicals, programmed cell death, tissue death, and self-degradation of cells [1,2,4].

Following CNS injury, oligodendrocytes interact with astrocyte cells at the scar tissue's periphery. This interaction leads to the generation of oligodendrocyte precursor cells (OPC). OPC cells subsequently secrete NG2, also known as chondroitin sulfate proteoglycan (CSPG) 4 [2]. NG2 cells can regulate cell distribution, exhibit the potential to differentiate into various cell types, and contribute to plasticity in the spinal cord and brain [5]. This study demonstrates that it promotes the activation of glial cells and the commencement of scar tissue development [1]. Gliosis, which refers to the formation of scar tissue, is a contributing component that hinders the growth of axons following chronic spinal cord injury [6,7].

SCI-induced secondary damage leads to further neuronal cell loss by apoptosis cell death mediated by intracellular caspase proteases [8]. Activating the caspase-3 proenzyme triggers the death of nerve cells in SCI during the chronic phase [4,9]. Caspase-3, upon cleavage, becomes an active fragment that plays a crucial role in promoting apoptosis. It is considered the final component in multiple apoptotic pathways [10]. The study by Yuan et al., in 2017 revealed a significant rise in caspase-3 mRNA and protein expression in rats stimulated with SCI [11]. Post-SCI pathological changes indicate that inflammatory reactions and immunological responses are not confined just to the CNS but can extend throughout the entire body. Interleukin-10 (IL-10) is a type of cytokine that has anti-inflammatory properties. It is produced by various types of cells, including macrophages, B cells, astrocytes, and microglia. The levels of IL-10 reached their highest point on the seventh day following SCI induction [12]. Elevating IL-10 levels has demonstrated beneficial effects on clinical outcomes in stroke, autoimmune encephalomyelitis, and SCI models [12–14]. Following SCI injury, a subsequent cascade of injuries occurs, leading to specific alterations in the histopathological presentation. These changes include an expansion of nerve tissue damage, Wallerian degeneration, microglial scar formation, and cavities development. The severity of neurological impairments is increased by the intensification of histopathological characteristics [7].

Moleac (MLC) 901 is an enhanced phytopharmaceutical that represents an advancement over its predecessor, MLC601 (also known as *Danqi Piantang Jiaonang/DPJ*). Research indicates that MLC901, which consists of a blend of active components, comprises crucial compounds that can generate favorable conditions for the growth and specialization of progenitor cells [15]. The extensive utility of MLC901 administration in facilitating stroke rehabilitation [16]. Multiple experimental and clinical investigations have demonstrated the efficacy of giving MLC901 in stroke cases. Studies investigating the isolation of cerebral cortex cells following the production of stroke have shown that the administration of MLC901 has a neurogenic effect. It means it promotes the growth of a more intricate network of dendrites and axon arborizations and the branching of neurites [17,18]. It also protects the brain from damage (neuroprotective), promotes the growth of new brain cells (neurogenesis), and increases the connections between brain cells (synapses) [19]. In addition to its use in stroke treatment, the efficacy of MLC901 as a supplementary therapy is also being investigated in the context of neurotrauma, dementia, and chronic pain [20]. MLC901 has been safe and improved the patient's motor function outcomes [21]. The neuroprotective effect is achieved by decreasing the permeability of blood vessels, which is accomplished by reducing the expression and levels of vascular endothelial growth factor (VEGF) in the bloodstream [22].

The administration of MLC901 is anticipated to benefit cellular processes in chronic phase SCI through many pathways of multiple grades. The MLC901 formulation contains seven out of the nine active ingredients, namely Astragali Radix (AR), Radix Salviae Miltorrhizae (RSM), Radix Paeoniae Rubra (RPR), Rhizoma Chuanxiong (RC), Angelicae Sinensis Radix (ASR), Carthamus Tinctorius (CT), and Radix Polygalae (RP). These ingredients have been scientifically proven to contribute to different secondary injury mechanisms in SCI. The components of MLC901 are recognized for their ability to inhibit apoptosis through several pathways. These include activating the P13K/AKT (AR, RC, and ASR) pathway, reducing Caspase-3 (RPR, RC, and CT), increasing BCL-2 (RC, and CT), and decreasing Bax (CT). The impact of the constituents of MLC901 on the inflammatory process is mediated through a specific mechanism. Enhancing IL-10 (RC) reduces TNF-A (AR, and RC), suppresses the NF-KB (AR, RSM, and ASR) pathway, lowers the signal-mediated TLR (RPR) activation, activates MKP-1 (AR), reduces MPO (ASR), and activates trkB/CREB (RP) signals. AR inhibits the GLIA reactivity process by decreasing AQP4. The component enhances myelin regeneration by stimulating neurogenesis, via activation of the BDNF/TRKB/ERK pathway. These cellular processes can improve the histological results of the spinal cord and the motor function of the Wistar rats post-induction SCI degree of weight in the chronic phase [18,23]. While we do not directly assess the chemicals inside

MLC901, we acknowledge that each of these compounds, as shown by numerous sources, contributes to the development of chronic pathogenesis. Currently, there is a lack of research examining the impact of MLC901 on inflammation, gliosis, and apoptotic pathways in chronic-phase SCI. This study aimed to investigate the effect of MLC901 administration on NG2 expression, caspase-3 expression, IL-10 levels, histopathological characteristics, and motor function in Wistar rats after severe spinal cord injury in the chronic phase.

## 2. Materials and methods

### 2.1. Design study

This research is true experimental research with a randomized post-test-only control group design in Fig. 1. The study was conducted at the Integrated Biomedical Laboratory. The necessary preparations for conducting research and administering medication were completed within the Laboratory Animal Unit of the Faculty of Medicine Universitas Udayana. The immunohistochemical investigation was conducted at the Histology laboratory. The enzyme-linked immunosorbent assay (ELISA) examination was conducted at the Clinical Pathology laboratory. The study lasted approximately three months, from February to April 2023. We obtained research permission from the Research Ethics Committee Faculty of Medicine, Universitas Udayana, to protect the basic rights and welfare of the subject of the research and to assure that the research operates by the International Conference on Harmonization - Good Clinical Practice (ICH -GCP) guidance and other applicable laws and regulations with registration number 27/UN14.2.2.VII.14/LT.2023.

### 2.2. Animals care

The subjects utilized in this study were male Wistar rats (*Rattus norvegicus*), who were in good physical condition and ranged in age from two to three months. A cohort of 18 rats was utilized for the study, with each group assigned a random allocation of six rats as subjects. These rats had a body weight ranging from 150 to 200 g. The experimental animals' health can be assessed by observing their level of agility, absence of lethargy, cleanliness of their skin, and absence of wounds, as well as the brightness and lack of glazing in their eyes. The study commenced by subjecting the experimental animals to a period of acclimatization to their surroundings for one week, during which their body weight was assessed. The laboratory setting where rats are housed for research is characterized by cleanliness, dryness, and enough air circulation. The rats were provided with aseptic food and water and housed in rats enclosures subjected to a 12-h light-dark cycle. The ambient conditions in the room were maintained at a temperature of  $22 \pm 2^\circ \text{C}$  and a humidity level of  $50 \pm 10\%$ .

### 2.3. MLC901 doses

The suggested daily dosage of MLC901 for adult individuals is two capsules, taken thrice daily. The MLC901 capsule has a total of 400 mg of active ingredients. The recommended daily dose for adults is 2400 mg, calculated by taking 400 mg six times a day. Calculation of MLC901 dose according to Nair and Jacob's (2016) methodology [24]. The author conducted experiments using rats models weighing 150 and 200 g and observed a ratio of 6.2. The equivalent dosage for mice relative to humans is calculated as 40 mg/kg multiplied by 6.2, resulting in 248 mg/kg. The weight of mice is 200 g. Hence, the daily dosage of MLC901 is calculated as 0.2 multiplied by 248, resulting in 49.6 mg. The MLC901 capsule contains 400 mg of active components dissolved in 12 ml of normal saline, resulting in a solution with a concentration of 33.33 mg/ml. The solution was vigorously stirred for 1 h at  $37^\circ \text{C}$  and then passed through a filter with a pore size of  $0.22 \mu\text{m}$  [18]. The author opted for the administration of MLC901 orally using a sonde. The amount of MLC901 delivered to each rat experimental animal weighing 0.2 kg may be calculated based on the solution concentration. It is determined by multiplying the animal's weight (0.2 kg) by the concentration of the solution (248 mg) and dividing the result by 33.33. This calculation yields a volume of 1.48 ml for a daily dosage of 1.5 ml of MLC901, administered three times at 0.5 ml each [24].

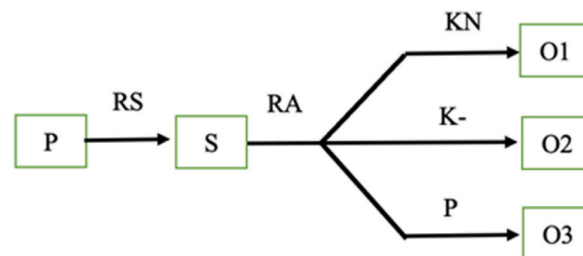


**Fig. 1.** The randomized post-test only control group. P = Population. S = Sample. RS = Random Sampling. RA = Random Allocation. KN = Normal control group (subjects underwent laminectomy surgery without induced spinal cord injury) K- = Negative control group (subjects received induction of severe spinal cord injury in the chronic phase) P = Treatment group (subjects received induction of severe SCI in the chronic phase, and treatment with MLC901). O1 = Normal control group post-test. O2 = Post-test negative control group. O3 = Post-test treatment group. The post-test results from observations in the form of NG2 expression, caspase-3 expression, interleukin-10 levels, histopathological features of the spinal cord, and motor function on the seventh day.

2.4. The protocol for the oral administration of MLC901

Following the prescribed dosage, the initial step involves gathering the necessary tools and supplies, such as plastic sondes and MLC901. The oral administration protocol for MLC901 involves the use of a probe [25]. Determine the accurate measurement of the sonde's length. The optimal length of a sonde is determined by measuring the distance from the inferior border of the oral cavity to the sternum. Ensuring appropriate length is crucial in mitigating the risks of aspiration and perforation. Typically, adult rats weighing 200 g necessitate a probe length measuring 75 mm and a diameter of 2.3 mm.

2.5. The provision of treatment

Before the surgical procedure, the rats were administered anesthesia with an intramuscular injection of ketamine by the researcher and laboratory assistant. The rats were positioned in a pronation stance and labeled with transverse markings on their upper and lower extremities. The distance between these two lines is divided into three equal pieces using two additional transverse lines to obtain the top, median, and lower parts. A surgical procedure involved the creation of an incision measuring 2.5 cm in length, originating 1 cm below the demarcation point between the upper and median regions. By utilizing this surgical incision, it will be possible to effectively see the thoracic (T9-11) region of the rat. Blunt and sharp dissection techniques separate the muscles enveloping the lamina and pedicle in the T9-11 region, creating a gap between the adjacent vertebrae. The laminectomy technique can be

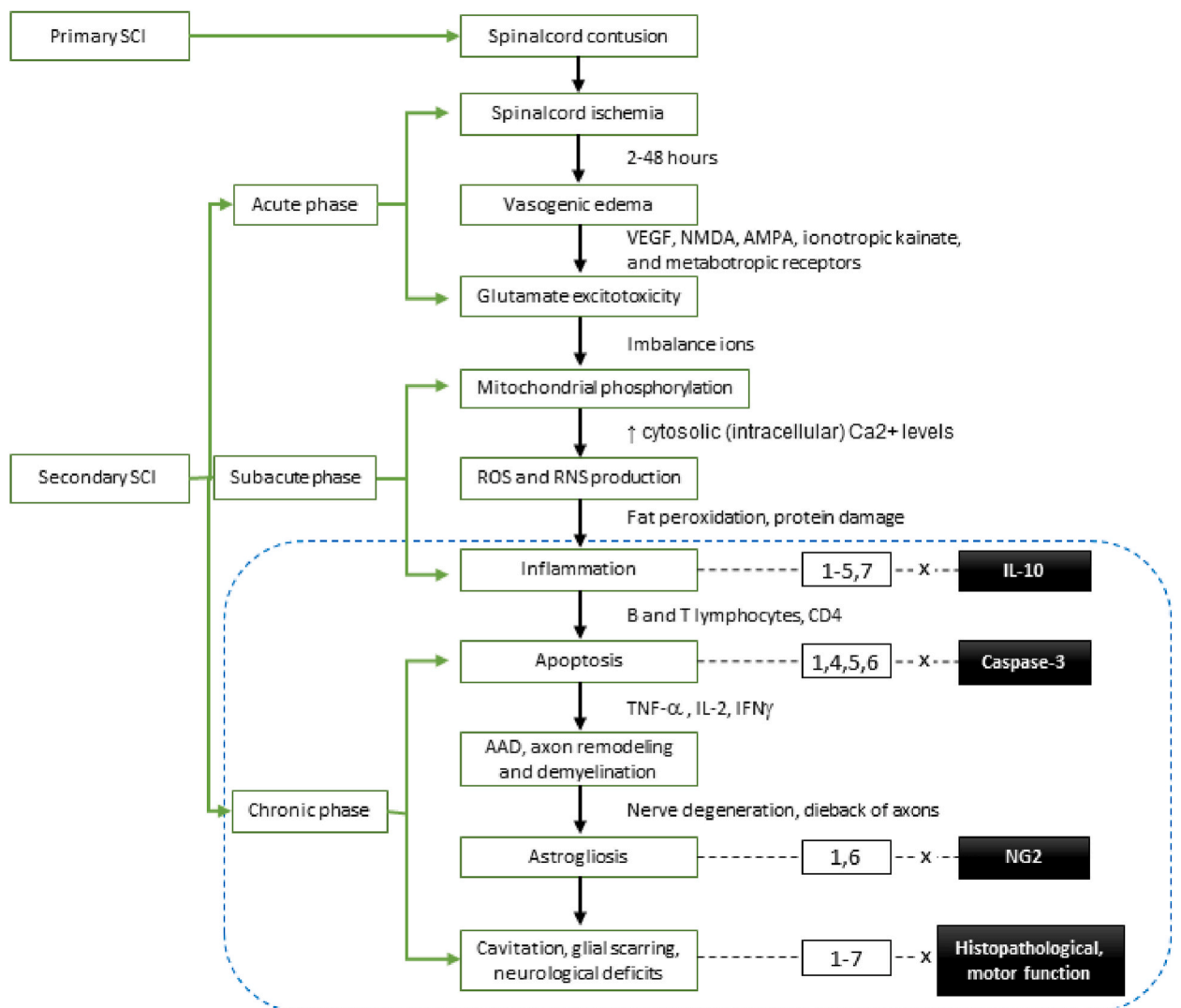


Fig. 2. The MLC901 component influences several pathophysiological pathways, including: 1 = *Astragali radix* (AR), 2 = *Radix salviae miltorrhizae* (RSM), 3 = *Radix paeoniae rubra* (RPR), 4 = *Rhizoma chuanxiong* (RC), 5 = *Angelicae sinensis radix* (ASR), 6 = *Carthamus tinctorius* (CT), dan 7 = *Radix polygalae* (RP).

performed by incising the lamina bilaterally through this aperture. Following a laminectomy procedure, an image is presented depicting the region of the spinal cord that has been exposed. A thoracic laminectomy procedure was conducted on all groups (KN, K-, and P) included in the study. Subsequently, the contusion-type SCI induction was performed in both the K- and P-groups [26]. Later, the rats were immobilized to ensure proper positioning while enabling sufficient visibility of the spinal cord without needing to open the dura mater. A 10-g force is released in free fall from a vertical distance of 50 mm using an Impact Tester until it with contacts the exposed section of the spinal cord. The incision wound is sutured using superficial fascia sutures, followed by a skin stapler to close the skin.

Before wound closure, the surgical wound is treated with gentamycin 0.3%, a topical antibiotic. The integumentary system is sealed using sterile gauze and a bandage on both ends. The complete sequence of procedures and therapies is conducted with scrupulous adherence to the principles of asepsis. Group P received treatment in oral administration of MLC901 at a dosage of 0.5 ml, with a solution concentration of 33.33 mg/ml. The administration of MLC901 commenced 2 h after the induction of SCI, occurring thrice daily and persisting until the conclusion of the seventh day.

We categorize chronic stages according to the origin and development of diseases from various sources. The chronic phases are distinguished by the presence of inflammatory delay (IL-10), apoptosis (Caspase-3), axon remodeling and demyelination (NG2), astrogliosis (NG2), cavity formation, glia grated tissue and neurological deficits (histopathological features and motor function assessed by BBB score). These effects reach their maximum intensity 7 days [2,27,28] after the contusion [2,26,29] refer to the diagram displayed in Fig. 2. In the chronic phase, spinal cord damage leads to reactive gliosis, characterized by hypertrophy and an excessive increase in astrocyte proliferation. The NG2 glycoprotein is a proteoglycan that is an essential component of the cell membrane of oligodendrocyte cell progenitors, also known as NG2 cells or CSPG4. The activation of TNFR2, FGF2, and GGF2 pathways following SCI leads to heightened TNF- $\alpha$  signaling, significantly promoting the proliferation of NG2 cells while simultaneously inhibiting their differentiation. The proliferation of NG2 glial cells can rise by a maximum of six times, precisely till day eight after spinal cord injury, in correlation with heightened astrocyte activity. Glia-NG2 cells have a role in inflammation by upregulating the production of several pro-inflammatory chemokines, cytokines, and MMPs. They also raise the levels of IL1B and CCL2. Additionally, they respond to IL-17 signals by activating Act1, activating NF $\kappa$ B. Moreover, glia-NG2 cells attract macrophages. A higher quantity of NG2 glial cells in reaction to long-term SCI plays a role in glial scar tissue development. The presence of fully developed glial scar tissue acts as a biological obstacle that might impede the recovery process of SCI [5,30,31].

Apoptosis is categorized into two pathways: extrinsic, which involves cell death receptors, and intrinsic, which involves mitochondria. The initiation of cell death receptors, such as the Fas receptor and TNF- $\alpha$ , activates the extrinsic apoptotic pathway in SCI. Fas triggers the activation of FADD, which then promotes the binding of the TNF- $\alpha$  ligand to its receptor (TNFR). This results in the activation of TNFR-associated death domain protein/TRADD and procaspase-8, ultimately leading to an upregulation of Caspase-3. The intrinsic route operates independently of receptor mediators, disrupting the equilibrium of intra and extracellular proteins, which triggers the activation of Caspase-3 and Caspase-9 and the release of cytochrome C [1,4].

The inflammatory responses following SCI are not confined solely to the spinal cord but can also extend to the systemic level. Consequently, elevated amounts of inflammation-related cytokines are also present in the bloodstream. Upon encountering inflammation, microglia/macrophages undergo activation and subsequently damage the blood-spinal cord barrier. The presence of macrophages in the spinal cord during SCI arises from the entry of monocytes (microglia) from the bloodstream and their local infiltration. Monocytes and Th2 cells produce interleukin-10, suppressing the release of IL-2, TNF- $\alpha$ , and GM-CSF cytokines from Th1 cells. Astrocytes, oligodendrocytes, microglia, and nerve cells all possess IL-10 receptors [1].

Alterations in the histological appearance of the spinal cord characterize SCI in the chronic phase. A contusive injury results in extensive neuronal and glial cell death, swelling, damage to both ascending and descending axons, and rupture of blood vessels. In the chronic phase of SCI, the remaining tissue is characterized by several cavities of different sizes. These cavities are surrounded by glial-vascular complexes acting as boundaries [32,33].

## 2.6. Assessment of motor function

On the seventh day, the assessment of motor function was conducted utilizing the Basso, Beattie, and Bresnahan (BBB) score [29]. Before the surgical procedure, the rats had a training regimen wherein they were acclimated to an open-field environment. This open field was constructed using circular plastic, with a smooth surface preventing slippage. The dimensions of this open field were as follows: a diameter of 90 cm and a wall height of seven cm. The implementation of brief open-field training and testing protocols resulted in a reduction in aggressive behavior and facilitated the rats acclimation to the open-field environment. Following the rat's continual movement in an open field, the examiner proceeded to provide a 4-min assessment session utilizing the BBB locomotive rating scale. All samples exhibiting complete injury cannot be analyzed for motor sparing in the research study due to the absence of an available modality. We used observer blind study to provide care for animals, administered therapy, and evaluated changes in study subjects without disclosing which samples have been treated and which have been assigned to the control group.

## 2.7. The tissue collection and histopathological preparations

The tissue section obtained from the microtome is subsequently transferred onto an object glass and subjected to a deparaffinization process, which involves separating paraffin from the tissue. The procedure involves sequentially immersed the tissue incisions in xylol for 2 min on three occasions. Subsequently, the incisions are consecutively transferred to ethanol solutions with decreasing concentrations. Initially, the incisions are immersed in 100% ethanol for 1 min on three occasions, followed by immersion in 95% ethanol for

1 min on two occasions. Finally, the incisions are immersed in 90%, 80%, and 70% ethanol solutions for 1 min each. Subsequently, the specimen should be thoroughly rinsed with tap water for approximately 5 min. It should then be immersed in Harris Haematoxylin for 6 min, followed by another round of water rinsing. Subsequently, the specimen should be immersed in a solution of 1% acidic alcohol for 3–5 dips and once again rinsed with water. The sample was immersed in ammonia water until it achieved a blue coloration. Subsequently, it was submerged in eosin solution, followed by sequential immersions in 95% ethanol for two 1-min intervals and in xylol for three 2-min intervals. Later, the mounting process was conducted using a xylene-based medium known as Entellan, followed by the placement of cover glass. The prepared sample was then subjected to microscopic examination.

The tissue is submerged in a 10% phosphate buffer formalin solution for one day. Next, the tissue soaked in alcohol solutions of increasing concentrations: 30%, 40%, 50%, 50%, 80%, 80%, and 96%, each for 25 min. In addition, the tissue is immersed in the Xylene Clearing Agent for 1 h on three separate occasions until it becomes transparent. Following infiltration at a frequency of three times per hour using pure paraffin, the tissue is then immersed in liquid paraffin to solidify into a block within roughly 3 h. This allows for easy slicing using a microtome. The tissue is sliced using a microtome into sections that are five  $\mu\text{m}$  thick. These sections are then affixed to glass objects coated with an adhesive substance like poly-lysine. The samples are after that placed in an incubator at a temperature of 60 °C for a duration of 2 h.

## 2.8. Euthanasia samples

The Wistar rats selected for sampling on the seventh day were then euthanized through the neck dislocation technique. The utilization of experimental animals is conducted according to research ethics guidelines, as stipulated by the Helsinki Declaration. It was approved by the Research Ethics Committee of The Faculty of Medicine, Universitas Udayana, and The Scientific Research Coordinator in The Health Sector of Universitas Udayana. Post-mortem animal care is often conducted after the study process, wherein the deceased animals are appropriately contained within paper or plastic bags, subjected to incineration in an incinerator, and interred.

## 2.9. Analysis of NG2 expression

NG2 was stained using the Dako EnVision®+ Dual Link System-HRP (DAB+) Kit and immunohistochemical polymer staining. Before painting, slides are deparaffinized and rehydrated. The slides are immersed in xylene twice for 5 min, then in 100% ethanol, 96% ethanol, 70% ethanol, and PBS for 2 min.

Antigen retrieval follows, where the slide is immersed in TE buffer and microwaved for 10 min at 700 W and 10 min at 240 W. After cooling, the slide is rinsed with PBS for 5 min. After 15 min in a plastic container with 0.3% H<sub>2</sub>O<sub>2</sub>, endogenous peroxidase activity was suppressed. After that, the samples were washed twice with PBS for 5 min. A 200  $\mu\text{L}$  aliquot of 5% FBS solution was incubated at room temperature for 15 min. The aliquot container was closed during incubation. After two 5-min PBS washes, 200  $\mu\text{L}$  of 1:100 diluted primary antibody was added and incubated in a sealed container for two nights. After overnight, rinsed each glass jar with PBS for 5 min twice with agitation. Apply labeled polymer-HRP to the slide and incubate for 30 min in a sealed container. The polymer-HRP conjugate contains tagged goat anti-rat antibodies that bind to NG2 antibodies. Conjugation with an HRP-labeled polymer labels antibodies. The samples were washed twice with PBS in a glass jar for 5 min with occasional shaking. The slide is covered with DAB chromogen substrate, which reacts with HRP enzyme on polymer coupled with anti-rat antibodies. This response turns HRP-containing cells brown, indicating NG2.

Next, apply DAB until a brown tint is attained, wash with PBS to guarantee cleanliness, and dry. Haematoxylin Meyer was then added and incubated for 5 min. The sample was rinsed with running water for 5 min and twice with dH<sub>2</sub>O for 5 min. Next, immersed in 70%, 95%, and 100% alcohol solutions for 2 min, twice. After that, the specimen was submerged in xylene twice for 5 min. Entellan, a xylene-based mounting solution, was used to attach the slides and add cover glass. The preparations were photographed with an Olympus CX41 microscope OptilabPro camera and saved as a JPEG file. Photographs were taken of NG2-expressing cells. These brown-cytoplasmic cells were measured to assess their abundance. We further examine NG2 utilizing the Elabscience ELISA kit.

## 2.10. Analysis of Caspase-3 expression

Caspase-3 staining uses the Dako EnVision®+ Dual Link System-HRP (DAB+) Kit. Slides are deparaffinized and rehydrated before painting. The slides were immersed in xylene two times for 5 min. After that, the slides are immersed in 100% ethanol for 2 min and then 96% for 2 min. Two minutes in 70% ethanol and two in PBS were also applied to the slides. Then, antigen retrieval occurs. After immersed the slides in Tri Sodium Citrate buffer solution, they are microwaved for 5 min at 800 Watts and 10 min at 400 Watts. Let the slides cool before washing them twice with PBS for 5 min. In a plastic container, 3% H<sub>2</sub>O<sub>2</sub> was used to suppress endogenous peroxidase for 30 min. The samples were then washed twice with PBS for 5 min. A 5% FBS solution of 100  $\mu\text{L}$  was incubated at room temperature for 30 min in a sealed container.

HRP-containing cell nuclei are brown, indicating Caspase-3. Applying DAB until a brown tint is obtained, washing with PBS to assure cleanliness, and drying are the next steps. After that, Haematoxylin Meyer was incubated for 5 min. Running water was used for 5 min, followed by two 5-min distilled water rinsed. Repeat the process twice with a 2-min immersion in 70%, 95%, and 100% alcohol solutions. The item was then submerged in xylene twice for 5 min. The slides were mounted using Entellan, a xylene-based medium, and then covered with a cover glass. The preparations were saved as a JPEG file after utilizing an Olympus CX41 microscope and OptilabPro camera with OptilabPro software. Caspase-3-expressing cells were photographed. These cells were counted and identified by their brownish nuclei. We further examine Caspase-3 utilizing the Elabscience ELISA kit.

### 2.11. The examination of interleukin-10 levels

Rats blood extraction through the retroorbital plexus of the eye. To overcome the blinded researcher, we need assistance from a trained animal handler. Retroorbital is highly beneficial, as it just needs one technician and allows for the rapid collection of samples from several animals without affecting their integrity [34]. Microhematocrit is gently scraped along the medial canthus of the eye to reach the optic foramen. The microhematocrit is then rotated to injure the plexus. This investigation used the Elabscience ELISA kit. Reagent preparation includes: Reagents should be equilibrated to room temperature (18–25 °C) before use. Follow microplate arrangement protocols and warm for 15 min before measuring optical density (OD). Remove the solution from each well and add 350  $\mu$ L of wash buffer. Immersed the object in a liquid medium for one to 2 min, then aspirated or poured the liquid from each aperture. A clean, absorbent paper should be used to dry the object. Note that a microplate washer can be used for this and other similar washing processes. Stir in 100  $\mu$ L HRP. Link each well to the working solution. Place plate sealer on the surface. Incubate the sample at 37 °C for 30 min.

Decant or aspirate the solution from each well and wash five times as instructed. Add 90  $\mu$ L of Substrate Reagent to each well. After applying a new plate sealer, incubate at 37 °C for 15 min. Reduce light exposure to the plate. The reaction period may be altered to match the color change rate but should not exceed 30 min. To each well, add 50  $\mu$ L of Stop Solution. As with the media solution, the stop solution should be added progressively. Use a 450 nm microplate reader to measure each well's OD.

### 2.12. The histopathological examination of the spinal cord

The histological appearance of the spinal cord samples was assessed following the induction of SCI, focusing on measuring the induced lesion's size at the induction site. The microscope is initially set to a magnification of 40 $\times$  to conduct a general evaluation. The magnification was enhanced to 100 to observe the cellular structures. The histological appearance of the spinal cord serves as a valuable reference for evaluation, particularly concerning the measurement of the size of the cavity. Additional characteristics to consider are the occurrence of hemorrhaging, deterioration of myelin, and the existence of syringomyelia inside the transverse region of the spinal cord. Quantitative measurements for the cavitation diameter were obtained using the Image Raster application.

### 2.13. Statistical analysis

This study analyzes data with SPSS 23.0 for Macintosh. The 95% confidence interval p-value  $\leq 0.05$ . In the three groups with a

**Table 1**

Characteristics of research subjects in the three groups.

Variable (N = 18)	Group	Median (IQR)	Mean $\pm$ Std	p-value
BW day-0	KN		193.97 $\pm$ 21.73	0.053
	K-		182.30 $\pm$ 11.30	0.311
	P	191.30 (33.88)		0.045*
BW day-7	KN		205.55 $\pm$ 21.49	0.078
	K-		184.88 $\pm$ 11.29	0.910
	P		207.81 $\pm$ 37.23	0.460
Temperature day-0	KN		36.81 $\pm$ 0.52	0.362
	K-		36.73 $\pm$ 0.60	0.100
	P		37.01 $\pm$ 0.32	0.164
Temperature day-7	KN		36.95 $\pm$ 0.67	0.469
	K-		36.63 $\pm$ 0.66	0.622
	P		36.40 $\pm$ 0.50	0.240
BBB score day-1	KN	20.00 (0.25)		<0.001*
	K-		0.83 $\pm$ 0.75	0.212
	P		0.67 $\pm$ 0.82	0.091
BBB score day-7	KN	20.50 (0.55)		0.004*
	K-		7.00 $\pm$ 1.55	0.456
	P		14.50 $\pm$ 1.38	0.191
Improved BBB score	KN		0.67 $\pm$ 0.81	0.091
	K-		6.17 $\pm$ 1.72	0.830
	P		13.83 $\pm$ 1.32	0.514
IL-10 level (pg/mL)	KN		2.32 $\pm$ 0.74	0.823
	K-		2.01 $\pm$ 1.09	0.583
	P		10.98 $\pm$ 9.69	0.265
NG2 expression	KN		2.10 $\pm$ 1.86	0.308
	K-		130.02 $\pm$ 47.53	0.072
	P		78.02 $\pm$ 12.26	0.562
Caspase-3 expression	KN		4.85 $\pm$ 1.77	0.390
	K-		160.34 $\pm$ 16.50	0.210
	P		65.45 $\pm$ 12.98	0.061

Note: \*Shapiro-Wilk test: p value  $\leq 0.05$  = significant; IQR= Interquartile range; BW= Body weight (gr); BBB= Basso, Beattie and Bresnahan, Locomotor activity evaluation; NG2 (H-score); Caspase-3 (H-score); IL-10 = Interleukin-10.

normal distribution and homogeneous data variance. The One-way ANOVA multiple comparison classical test was employed to compare mean NG2 expression, caspase-3 expression, IL-10 levels, and improved BBB score. A post hoc test using the LSD test was utilized to compare groups after a significant One-Way ANOVA test ( $p \leq 0.05$ ). ROC analysis is used to set P- and K-group cavitation diameter cut-offs. ROC analysis yields AUC. Considerable difference in AUC  $>0.7$ ,  $p \leq 0.05$ . Next, determine cavitation diameter category sensitivity and specificity using the cut-off point. High sensitivity and specificity  $>0.8$  indicate accurate cavitation diameter prediction between groups. We also use a path analysis.

### 3. Results

#### 3.1. Characteristics in the three groups

The subjects were categorized into three groups based on their basic features: KN, K-, and P in Table 1. A random allocation was performed, assigning six rats to each group, resulting in a total sample size of 18 rats. The data presented in this study includes subject characteristics such as body weight (BW), body temperature, BBB score, NG2 expression, Caspase-3 expression, and IL-10 levels. We also analyzed the mean differences observed for each variable in Table 2.

#### 3.2. NG2 expression

The findings of this study indicate that the KN had the lowest average value of NG2 expression, specifically  $2.10 \pm 1.86$ . In contrast, the P group displayed a relatively higher mean value of  $78.75 \pm 12.26$ , while the K- group had the highest mean value of  $130.02 \pm 47.53$ . The test results indicated statistically significant variations in the NG2 expression variable ( $p \leq 0.05$ ) among the three groups in Table 2. Subsequently, a post-hoc analysis for NG2 in Table 3 was conducted using the Mann-Whitney test. The comparison test yielded statistically significant variations in NG2 expression among the following groups: KN and K-, KN and P, and K- and P ( $p \leq 0.05$ ). Immunohistochemical analysis (IHK) was conducted on the three experimental groups to assess the expression of NG2, as depicted in Fig. 3(A–D).

#### 3.3. Caspase-3 expression

The findings of this study indicate that the KN group had the lowest average Caspase-3 expression value, specifically  $4.85 \pm 1.77$ . In contrast, the P group had a comparatively higher mean value of  $65.45 \pm 12.98$ , while the K- group had the highest mean value of  $160.34 \pm 16.50$ . The data of the variability of Caspase-3 expression was observed to follow a normal distribution among the three distinct research groups. A one-way ANOVA test in Table 2 was employed for the comparison analysis. The test findings indicated a statistically significant disparity in the variable of Caspase-3 expression ( $p \leq 0.05$ ). Subsequently, the obtained data were further analyzed using post hoc testing, specifically the Least Significant Difference (LSD) test in Table 3. The findings from the LSD comparison test revealed statistically significant variations in the expression of Caspase-3 among the KN vs. K- groups, the KN vs. P groups, and the K- vs. P groups ( $p \leq 0.05$ ). IHK was performed on the three experimental groups to evaluate the expression of Caspase-3, as illustrated in Fig. 4(A–D).

#### 3.4. IL-10 levels

The P group had the highest average IL-10 level, specifically  $10.98 \pm 9.69$  pg/ml. In contrast, the KN group displayed a comparatively lower mean of  $2.32 \pm 0.74$  pg/ml, while the K- group had a mean of  $2.01 \pm 1.09$  pg/ml. The findings about IL-10 levels in the three study groups exhibited a normal distribution. The Levene test revealed that the data showed heterogeneity ( $p \leq 0.05$ ). The data did not exhibit homogeneity after undergoing the data transformation process, thus necessitating the selection of the Kruskal-Wallis test to conduct the comparison test in Table 3. The test findings indicated no statistically significant variations in the IL-10 level variable ( $p \geq 0.05$ ) across the three groups.

#### 3.5. Histopathological features of the spinal cord

In group K-, a distinct region of contusion (induced by SCI) is observed in the macroscopic examination of the spinal cord, in contrast to group P. Group P demonstrates a notable enhancement in the localization of the contusion; nevertheless, when assessed

**Table 2**  
Differences in NG2, Caspase-3 expression, IL-10 level, and BBB score in the three groups.

Variable	Mean	p-value
Ekspresi NG2	4.333	0.037*
Caspase-3 Expression	36854.447	<0.001*
IL-10 levels	4.020	0.056
Improved BBB Score	262.389	<0.001*

\* $p \leq 0.05$  = significant.

**Table 3**

Post-hoc test in NG2, Caspase-3 expression, and BBB score in the three groups.

Variable	Group	Mean Difference	p-value
NG2	KN vs. K-	-127.92	0.004*
	KN vs. P	-75.92	0.004*
	K- vs. P	52.00	0.037*
Caspase-3	KN vs. K-	-155.49	<0.001*
	KN vs. P	-60.60	<0.001*
	K- vs. P	94.89	<0.001*
BBB Score	KN vs. K-	-5.50	<0.001*
	KN vs. P	-13.12	<0.001*
	K- vs. P	-7.67	<0.001*

KN = normal control group (subjects underwent laminectomy surgery without induced SCI); K- = negative control group (subjects received induction of SCI in the chronic phase); P = treatment group (subjects received induction of severe SCI in the chronic phase, and treatment was given MLC901). P-value  $\leq 0.05$  = significant.

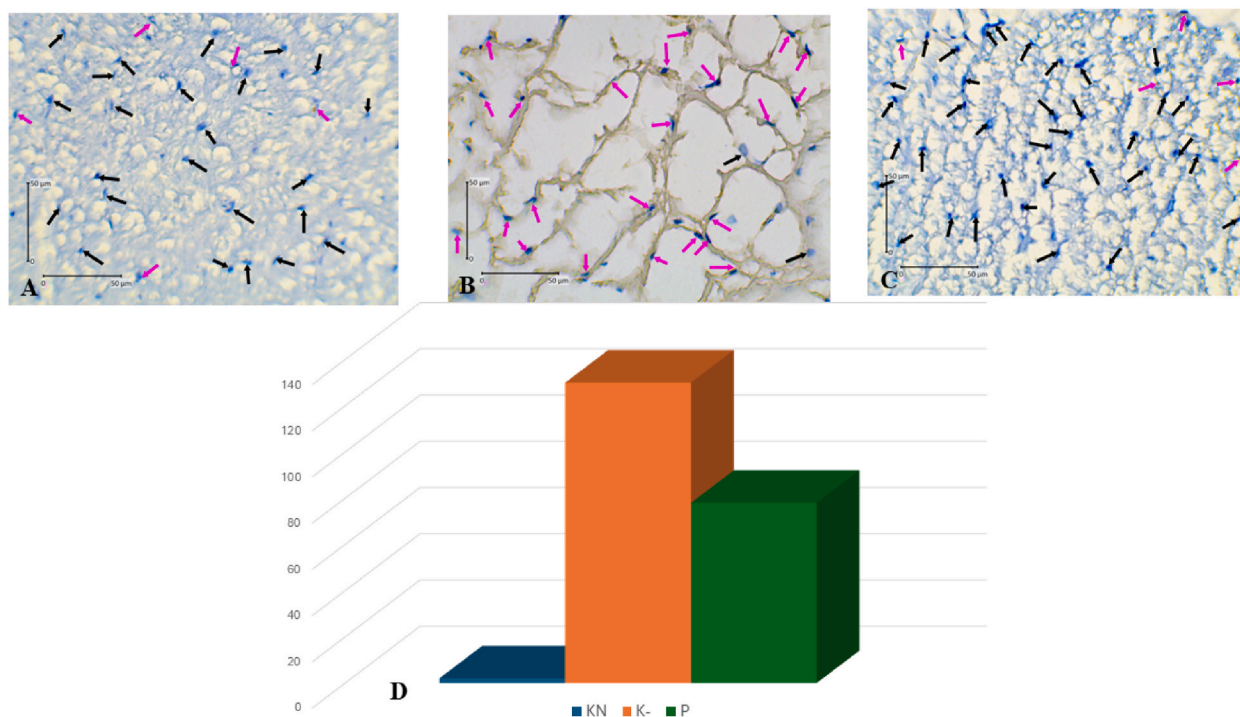


**Fig. 3.** The evaluation of NG2 immunostaining in spinal cord tissue involved quantifying the ratio of positively stained cells in the brown cytoplasm to the total number of cells. NG2 is present in the cytoplasm (shown by the pink arrow), whereas it is absent in the cytoplasm (indicated by the black arrow). Figure A = KN for the normal control group (subjects underwent laminectomy surgery without induced spinal cord injury); Figure B=K- for the negative control group (subjects received induction of severe spinal cord injury in the chronic phase), Figure C=P for the treatment group (subjects received induction of severe SCI in the chronic phase, and treatment with MLC901), and Figure D = The mean values of each group are computed based on the Elisa levels. (For interpretation of the references to color in this figure legend, the reader is referred to the Web version of this article.)

macroscopically, it fails to achieve a comparable level to that of KN. Histopathological images of the spinal cord were obtained from three distinct research groups. HE staining was employed to enhance the visualization of cellular structures. The photos were captured at magnifications of 40 $\times$  and 100 $\times$ . Fig. 5 depicts the axial cross-sectional view of the spinal cord in the KN, K-, and P groups, specifically seven days following the initiation of SCI symptoms. The spinal cord of the K-group exhibited significant damage, inadequate tissue differentiation, and distinct cavitation pictures. The P group's histological features of the spinal cord showed superior characteristics to the K- group. However, the extent of structural differentiation remained uncertain when compared to the KN group. Cavitation was observed in both the K- and P groups as a histological manifestation of spinal cord injury resulting from the induction of severe SCI in the chronic phase.

Nevertheless, the KN group did not exhibit any signs of cavitation. The average cavitation diameter in the K- group was found to be much greater, measuring  $179.28 \pm 31.68 \mu\text{m}$ , compared to the P group, which had a mean diameter of  $52.73 \pm 26.13 \mu\text{m}$ . Subsequently, a ROC analysis was conducted on groups K and P, utilizing the cavitation diameter data. The investigation yielded an AUC

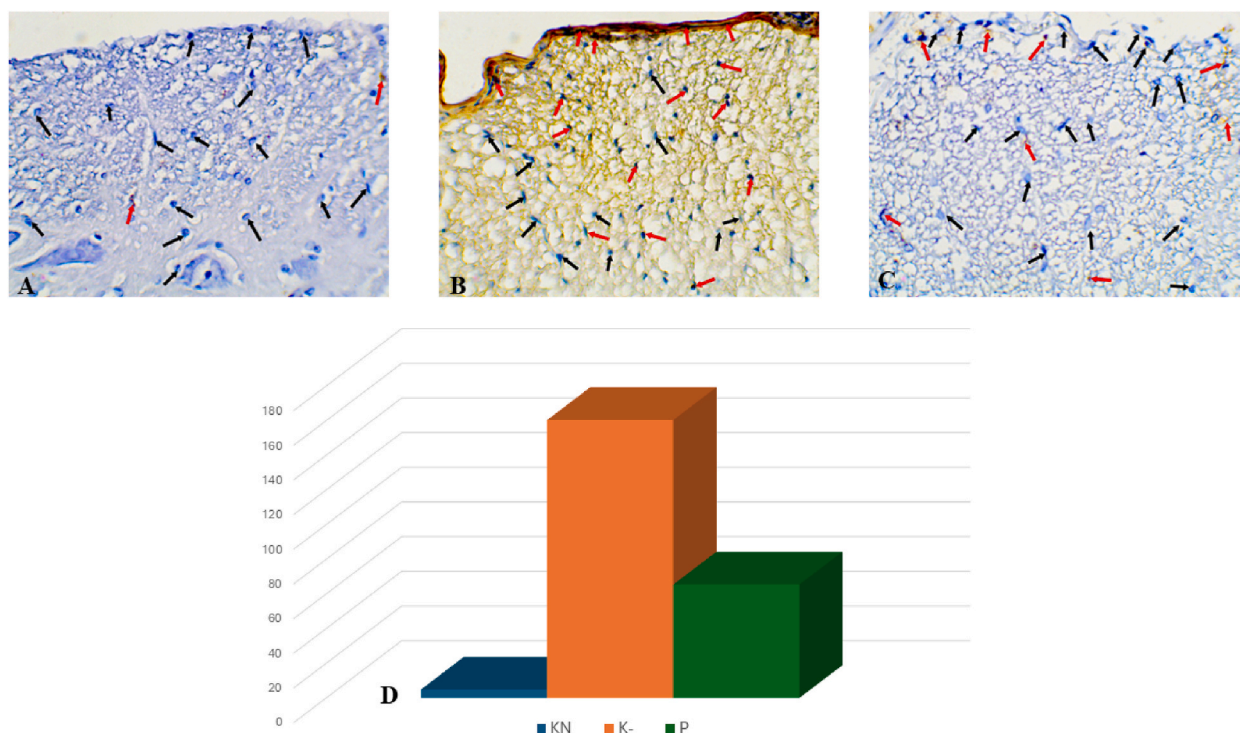


**Fig. 4.** The translocation of caspase-3 into the nucleus signifies the initiation of apoptosis. Caspase-3 is present in the nucleus, as indicated by the red arrow, and absent in the nucleus, as indicated by the black arrow. Figure A = KN for the normal control group (subjects underwent laminectomy surgery without induced spinal cord injury); Figure B=K- for the negative control group (subjects received induction of severe spinal cord injury in the chronic phase), Figure C=P for the treatment group (subjects received induction of severe SCI in the chronic phase, and treatment with MLC901), and Figure D = The mean values of each group are computed based on the Elisa levels. (For interpretation of the references to color in this figure legend, the reader is referred to the Web version of this article.)

value of 1.0, indicating perfect discrimination. The statistical significance of the data was established with a p-value less than 0.05. The test findings suggest that sensitivity and specificity are 100%, with a cavitation diameter value of 114.915  $\mu\text{m}$  as the designated cut-off in Fig. 6. Samples obtained in the chronic phase after the induction of SCI exhibit more severe spinal cord damage when the cavitation diameter is equal to or more than 114.915  $\mu\text{m}$ .

### 3.6. Motor function

Motor function was evaluated by measuring the increase in BBB score on the seventh day following the induction of SCI damage. The findings of this study indicate that the P group had the highest average rise in BBB score, specifically  $13.83 \pm 1.32$ . In contrast, the K- group had a comparatively lower mean increase of  $6.17 \pm 1.72$ , while the KN group had the lowest mean increase of  $0.67 \pm 0.81$ . It is well-established that the variable data used to enhance the BBB score exhibits a normal distribution. The Levene test results indicated homogeneous data ( $p \geq 0.05$ ). Hence, the One-way ANOVA test was employed for the comparative analysis in Table 2. The obtained test results showed a statistically significant disparity in motor function, with a p-value less than 0.05. Subsequently, the obtained data were further analyzed using post hoc testing, specifically the LSD test, as presented in Table 3. The findings from the LSD comparison test revealed statistically significant disparities in motor performance across three groups: KN and K-, KN and P, and K- and P ( $p \leq 0.05$ ). The initial BBB scores we described in Table 4.

### 3.7. Pathway analysis

A path analysis was conducted employing multiple linear regression analysis to elucidate the association between variables and determine the extent of interaction between the dependent and independent variables. Various iterations of linear regression are performed based on the chosen dependent variable and supplied variables. The analysis consisted of four distinct stages. The first stage involved evaluating the interaction pathway between MLC901 and IL-10. In the second stage, the assessment focused on MLC901 with Caspase-3, with IL-10 as a covariate. The research investigated the correlation between MLC901 and NG2 in the third phase while considering IL-10 and Caspase-3 as confounders. Finally, the fourth stage involved assessing the impact of MLC901 on increased BBB score, considering IL-10, Caspase-3, and NG2 as covariates. The findings of the path analysis are depicted in Fig. 7. The interaction pattern shown in Fig. 6 suggests an increase in the BBB score, which indicates SCI outcomes. The impact of MLC901 did not yield a

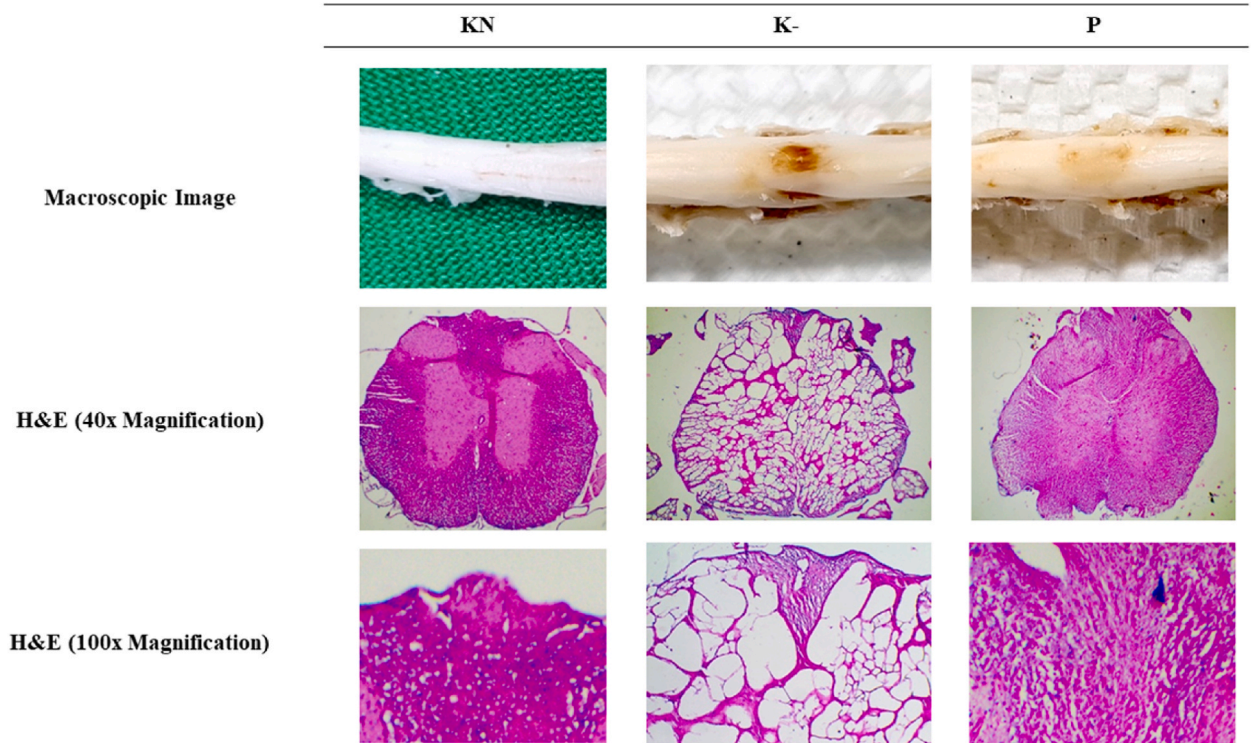


Fig. 5. Histopathological features of the spinal cord in the three groups.

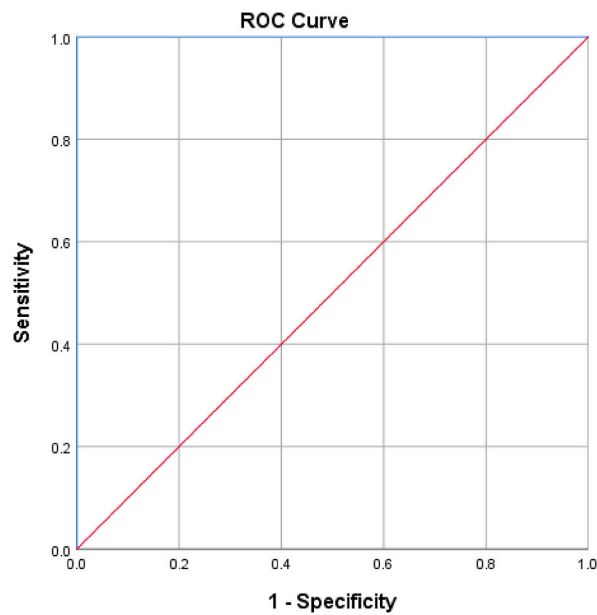


Fig. 6. ROC curve of cavitation diameter.

statistically significant increase in BBB ratings ( $B\ 2.446; p \geq 0.05$ ). MLC901 played a substantial influence in the upregulation of IL-10 levels ( $B\ 8.968; p \leq 0.05$ ), as well as the downregulation of Caspase-3 expression ( $B\ -52.000; p \leq 0.05$ ) and NG2 expression ( $B\ -94.892; p \leq 0.05$ ). The administration of MLC901 demonstrated a considerable improvement in BBB score, mediated mainly by the upregulation of NG2 and the indirect enhancement of Caspase-3 activity.

**Table 4**  
BBB score day-1 and day-7 for each sample group.

Group	BBB score day-1	BBB score day-7
KN1	19	21
KN2	20	20
KN3	20	20
KN4	20	20
KN5	20	21
KN6	20	21
K-1	1	5
K-2	1	6
K-3	0	9
K-4	2	8
K-5	0	13
K-6	1	15
P1	0	13
P2	1	15
P3	1	13
P4	0	14
P5	2	16
P6	0	16

KN = Normal control group (subjects number 1–6 underwent laminectomy surgery without induced spinal cord injury); K- = Negative control group (subjects number 1–6 received induction of severe spinal cord injury in the chronic phase); P = Treatment group (subjects number 1–6 received induction of severe SCI in the chronic phase, and treatment with MLC901).

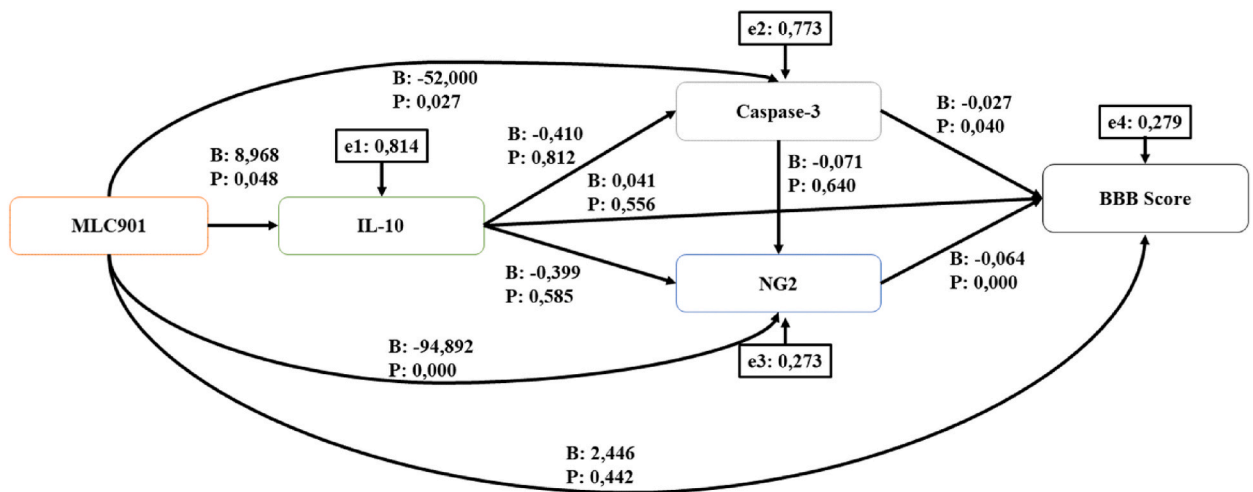


Fig. 7. Pathway analysis of MLC901 on research variables.

#### 4. Discussion

The regulatory function of the protein NG2 extends to the dispersion of cells throughout the central nervous system. Cells that express NG2 undergo differentiation and have a role in maintaining plasticity in the spinal cord and brain. The activation triggers the activation of oligodendrocytes, specialized cells responsible for forming OPC in conjunction with astrocytes. This collaborative process results in the production of NG2, a crucial component in the central nervous system. Cells that produce NG2 and the presence of local inflammation can disrupt the integrity of the blood-spinal cord barrier [35]. The peak rise in NG2 is observed on the eighth day following the start, particularly in the central region of the scar tissue. MLC901 also contributes to the regeneration of myelin and the growth of neurites via activating the BDNF/TrkB/ERK pathway. Neurite growth is crucial for reestablishing connections between nerve cells and synaptic connections [36]. Alleviate inflammation, enhance microcirculation, suppress nerve cell apoptosis, safeguard impaired nerve cells, and facilitate nerve healing and regeneration. Thus far, no investigation has been conducted to examine the correlation between MLC901 and the expression of NG2. Nevertheless, the use of mesenchymal stem cells in conjunction with MLC901 demonstrates significant clinical improvement in SCI, resulting in enhanced BBB scores in animal models such as rats [37].

Caspase-3 cleaves into active pieces to mediate apoptosis [10]. MLC901 significantly reduced caspase-3 expression seven days after severe SCI induction [10]. Most research examines MLC901 and caspase-3 expression. Analysis of rats with cerebral ischemia suggests

that MLC901 treatment lowers caspase-3 expression. MLC901 targets the mitochondrial-associated caspase-3 apoptotic pathway, according to the study. In the ischemic brain, Z-ligustilide dramatically reduced BAX and caspase-3 protein expression [30]. SCI-induced rats expressed more caspase-3 mRNA and protein than controls [11]. MLC901 contains “*Rhizoma chuanxion*” and “*Carthamus tinctoriu*” with *Ligustrazine* (tetramethylpyrazine/TMP) and SY [35]. SCI model cell culture research shows that TMP decreases ROS, modulates NO, enhances SOD, and greatly reduces MDA. In rats, TMP increases Bcl-2, reduces caspase-3, activates the P13K/Akt pathway, and prevents nerve cell death [38,39]. MLC901’s active component SY reduces apoptosis in rabbits after ischemia-reperfusion [9]. Neuroprotective SY intervention increases Bcl-2, inhibits Bax, and activates caspase-3. SY mechanism in SCI-induced inflammation by restricting TNF- $\alpha$ , suppressing the high mobility group box 1 protein-TLR4-NF- $\kappa$ B signal pathway, and lowering ROS [40]. MLC901 suppresses apoptosis and promotes neurite development by activating the BDNF/TrkB/ERK pathway. Neurite expansion is crucial to nerve cell-synaptic reconnection [36]. The MLC901 capsule is considered to include a chemical whose composition is thought to contribute to the mechanism of SCI, as indicated in Table 5.

In SCI, interleukin-10 inhibits secondary inflammatory reactions and cytokine expression. IL-10 receptor mRNA expression affects neuronal development [14]. MLC901 intake affects IL-10 levels in rats in stroke models. Microglia/macrophages are highly plastic cells that can express two opposing phenotypes: cytotoxic M1 polarization, which releases pro-inflammatory mediators (cytokines, ROS, proteinases), and repair-related M2 polarization [41]. The study found that MLC901 significantly boosted IL-4R $\alpha$  mRNA expression in brain microglia and monocytes, promoting protective and repair activities. MLC901 may help microglia switch from M1 to M2 [41]. IL-10 receptor binding activates the JAK/STAT signaling cascade, upregulating immunomodulatory genes. It then suppresses inflammation by inhibiting pro-inflammatory mediators, antigen presentation, and phagocytes. MLC901 contains RC with TMP alkaloids, Ferulic acid, senkyunolide I, and ligustilide, which interact with the ALB, AKT1, MAPK1, MMP9, and EGFR genes to reduce pro-inflammatory cytokines (IL-1 $\beta$  and TNF- $\alpha$ ) and increase IL-10 [35]. Pharmacological studies on the SCI model show that RC interacts with AKT1, MAPK1, MMP9, caspase-3, and EGFR genes [39,42]. Anti-inflammatory IL-10 inhibits caspase-3, cytochrome C activity, Bax, and Bcl-2 to suppress apoptosis directly. Through the NF- $\kappa$ B and AP1 pathways, interleukin-10 activates cytotoxic T and NK cells increases B cell MHC class II molecules, and switches Ig to IgG1, IgG3, and IgA. After SCI, IL-10 production increases to control the local inflammatory response and protect the penumbral nerve and glial cells [11].

According to previous research findings, fibroblasts and macrophages can be detected within the affected lesion and astrocytes in severe histological manifestations of SCI. Gliosis and collagen fibrosis manifest after the clearance of necrotic material [32]. The presence of vascular glial complexes hinders the occurrence of multilocus cavitation in tissue at the site of a lesion [33]. As in previous research, the histopathological characteristics of scar tissue in the spinal cord resulting from induced contusion were deemed suitable for examination in the K-group [31]. The typical spinal cord exhibits parenchyma characterized by astrocytes, oligodendrocytes, and glia-NG2 cells. Nevertheless, contusive injuries result in extensive loss of neurons and glial cells and damage to both ascending and descending axons due to stretching and rupture of blood vessels. Studies have demonstrated that the induced SCI group has a significant intraparenchymal cavity, encompassed by many reactive astrocytes with intensified acidophilic cytoplasm, a dark diminishing core, hemorrhage, and localized inflammation [4,43,44]. The findings of this study demonstrate that prolonged severe SCI results in tissue damage, significant cell death characterized by increased expression of Caspase-3, cytoplasmic presence of NG2, and a larger spinal cord cavitation in the K- group compared to group P. Upon administration of MLC901, the experimental group exhibited a decreased cavitation diameter compared to the control group K-, although it did not reach the same level as the positive control group KN. Spinal cords generated by SCI exhibited intraparenchymal cavitation and numerous reactive astrocytes characterized by high acidophilic cytoplasm, dark, shrunken nuclei, bleeding, and localized inflammation [43].

Multiple studies have investigated the effects of MLC901 on motor function [21,23,35]. The administration of MLC901 enhanced motor performance in a rats model of ischemic stroke for seven days [19]. The neuroprotective effects of MLC901 are attributed to its ability to activate KATP channels and decrease the expression of Bax protein. The administration of MLC901 has been shown to enhance the population of BrdU-positive progenitor cells and promote the process of basal neurogenesis. BDNF is a crucial regulator of neuronal viability and synaptic plasticity within the central nervous system. MLC901 likewise enhanced the expression of this molecule. The promotion of neuroprotection is facilitated by the Akt survival pathway and the activation of ATP channels [17,18,44]. According to a meta-analysis, the administration of MLC901 demonstrated significant improvements in infarct volume, brain BrdU expression, and neurological function as assessed by the Bederson Neurological Outcome Score in animal models of acute ischemic brain injury. MLC901 has been found to enhance the recovery process of acute ischemic brain injury [23]. The AIS examination demonstrated a 25% enhancement in AIS A and a 50% improvement in AIS B after administering conventional therapy with MLC901 [21].

The impact of the active constituents of MLC901 on gliosis, apoptosis, and inflammatory responses, potentially influencing motor performance. The process under investigation involves the inhibition of apoptosis through various mechanisms. These mechanisms include the combination of AR-ASR via the P13K/Akt pathway, the active ingredient in RPR, and the active ingredient in CT in the form of SY, which leads to an increase in Bcl-2 expression and the inhibition of Bax. The alkaloids derived from traditional medicinal plants (TMP) have been found to exhibit anti-inflammatory properties by reducing the levels of proinflammatory cytokines. It improves microcirculation and ultimately contributes to the reduction of tissue cavitation. Following the development of severe SCI damage during the chronic phase, the administration of MLC901 resulted in enhancements in cellular processes and motor function, as evidenced by an observed elevation in the BBB score.

The mechanism of action of MLC901 is believed to include many pathways, but it is not yet fully comprehended. The significance of the findings from this study lies in its ability to demonstrate the enhancements observed in NG2 expression, Caspase-3 expression, IL-10 levels, histological grade of the spinal cord, and motor function. Consequently, these data provide more support for the idea of SCI recovery. The administration of MLC90 has positive effects on motor function and histopathological outcomes of the spinal cord in the

**Table 5**

Exposure to the component and active ingredients in MLC901, the effect and mechanism of action in SCI.

MLC901 component	Active compounds	Effect	Mechanism
<i>Astragali radix</i> ( <i>Astragalus membrana-ceus</i> ) (AR) [45,46]	Isoflavonoid	Apoptosis, glia reactivity, inflammatory, neuroprotective, antioxidant	Activation of the P13K/AKT pathway, MKP-1 activation simultaneously weakens P38 and ERK, decreases AQP4, TNF- $\alpha$ , inhibits the NF- $\kappa$ B pathway, decreased SOD, MDA and GFAP expression.
<i>Radix salviae miltorrhizae</i> (RSM) [39,47,48]	Salvianolic acid	Inflammation, edema, oxidative stress	Inhibits ERK, inhibits the NF- $\kappa$ B path, decreases MDA expression.
<i>Radix paeoniae rubra</i> (RPR) [39,40, 47–49]	Paeoniflorin	Apoptosis, inflammation	Reducing Caspase-3, lowering TLR mediated signals.
<i>Rhizoma chuanxiong</i> (RC) [39,42]	Alkaloid Tetra-methylpyrazine, Ferulic acid, senkyunolide I, dan ligustilide	Apoptosis, inflammation	Increases BCL-2, decreases Caspase-3, activation of the P13K/AKT pathway, interacting with the ALB, AKT1, MAPK1, MMP9, and EGFR genes decreases proinflammatory cytokines (IL-1mit and TNF- $\alpha$ ) and increases IL-10).
<i>Angelicae sinensis radix</i> (ASR) [15,50]	Polysaccharides, Z-Stillicide, dan ferulic acid	Apoptosis, inflammation, regenerative	Activation of the P13K/AKT pathway, inhibits the NF- $\kappa$ B path, lowering MPO, helping the differentiation of stem cells.
<i>Carthamus tinctorius</i> (SY) [9,40,51]	Safflower Yellow	Apoptosis, myelin regeneration	Increasing BCL-2, lowering Bax and Caspase-3, triggers growth and expansion of neurite through the activation of the BDNF/TrkB/ERK pathway.
<i>Radix polygalae</i> (RP) [52, 53]	Sibiricose A5 dan 3,6'-disinapoyl sucrose	Inflammation	Activation of TrkB/CREB signals causes M2 dominance (increases IL-4, NGF, and BDNF).

chronic phase of severe SCI in Wistar rat animal models. These effects are achieved through biomolecular mechanisms that suppress the processes of gliosis, neuroapoptosis, and neuroinflammation. This study also demonstrates that the administration of MLC901 leads to an enhancement in the histological characteristics of the spinal cord following severe SCI during the chronic phase, as seen by a reduction in cavitation diameter. In addition, this study is limited in its scope as it did not assess the extended length of follow-up required to ascertain the potential for long-term advantages, nor did it thoroughly investigate the individual effects of each active component included in MLC901.

## 5. Conclusions

This study shows that MLC901 reduces degenerative processes (gliosis, apoptosis, and neuroinflammation) and improves morphological and functional results in chronically injured Wistar rats.

## Ethics statement

We obtained research permission from the Research Ethics Committee Faculty of Medicine, Universitas Udayana, to protect the basic rights and welfare of the subject of the research and to assure that the research operates by the International Conference on Harmonization - Good Clinical Practice (ICH -GCP) guidance and other applicable laws and regulations with registration number 27/UN14.2.2.VII.14/LT.2023.

## Data availability statement

All data generated and analyzed are included in this report.

## CRediT authorship contribution statement

**Dewa Putu Wisnu Wardhana:** Writing – review & editing, Writing – original draft, Resources, Project administration, Investigation, Formal analysis, Data curation, Conceptualization. **Sri Maliawan:** Validation, Formal analysis, Data curation. **Tjokorda Gde Bagus Mahadewa:** Formal analysis, Conceptualization. **Andi Asadul Islam:** Visualization, Validation, Resources. **I Made Jawi:** Methodology, Investigation, Formal analysis. **Anak Agung Wiradewi Lestari:** Investigation, Formal analysis, Conceptualization. **I Gusti Kamasan Nyoman Arijana:** Formal analysis. **Rohadi Muhammad Rosyidi:** Project administration, Methodology, Investigation, Conceptualization. **Sinta Wiranata:** Software, Resources, Project administration, Investigation, Data curation, Conceptualization.

## Declaration of competing interest

The authors declare that they have no known competing financial interests or personal relationships that could have appeared to influence the work reported in this paper.

## Acknowledgments and funding statement

The authors express their gratitude to Beasiswa Pendidikan Pascasarjana Dalam Negeri (BPPDN) by the Indonesian Ministry of Research, Technology and Higher Education who have provided support for this research.

## References

- [1] A. Alizadeh, S.M. Dyck, S. Karimi-Abdolrezaee, Traumatic spinal cord injury: an Overview of pathophysiology, models and acute injury mechanisms, *Front. Neurol.* 10 (2019) 282, <https://doi.org/10.3389/fneur.2019.00282>.
- [2] A. Anjum, M.D. Yazid, M. Fauzi Daud, J. Idris, A.M.H. Ng, A. Selvi Naicker, O.H.R. Ismail, R.K. Athi Kumar, Y. Lokanathan, Spinal cord injury: pathophysiology, multimolecular interactions, and underlying recovery mechanisms, *Int. J. Mol. Sci.* 21 (2020) 7533, <https://doi.org/10.3390/ijms21207533>.
- [3] Y. Kang, H. Ding, H. Zhou, Z. Wei, L. Liu, D. Pan, S. Feng, Epidemiology of worldwide spinal cord injury: a literature review, *J. Neurorestoratol.* 6 (2017) 1–9, <https://doi.org/10.2147/jn.s143236>.
- [4] F. Abbaszadeh, S. Fakhri, H. Khan, Targeting apoptosis and autophagy following spinal cord injury: therapeutic approaches to polyphenols and candidate phytochemicals, *Pharmacol. Res.* 160 (2020) 105069, <https://doi.org/10.1016/j.phrs.2020.105069>.
- [5] J. Eugenin-von Bernhardt, L. Dimou, NG2-glia, more than progenitor cells, *Adv. Exp. Med. Biol.* (2016) 27–45, [https://doi.org/10.1007/978-3-319-40764-7\\_2](https://doi.org/10.1007/978-3-319-40764-7_2).
- [6] J. Kjell, L. Olson, Rat models of spinal cord injury: from pathology to potential therapies, *Dis. Model. Mech.* 9 (2016) 1125–1137, <https://doi.org/10.1242/dmm.025833>.
- [7] C.S. Ahuja, S. Nori, L. Tetreault, J. Wilson, B. Kwon, J. Harrop, D. Choi, M.G. Fehlings, Traumatic spinal cord injury—repair and regeneration, *Neurosurgery* 80 (2017) S9–S22, <https://doi.org/10.1093/neuros/nyw080>.
- [8] Y. Zhang, Y. Wu, Y. Fu, L. Lin, Y. Lin, Y. Zhang, L. Ji, C. Li, Anti-Alzheimer's disease molecular mechanism of acori tatarinowii rhizoma based on network pharmacology, *Med. Sci. Monit. Basic Res.* 26 (2020) e924203, <https://doi.org/10.12659/MSMBR.924203>.
- [9] D. Zhou, B. Liu, X. Xiao, P. Dai, S. Ma, W. Huang, The effect of safflower yellow on spinal cord ischemia reperfusion injury in rabbits, *Oxid. Med. Cell. Longev.* 2013 (2013) 692302, <https://doi.org/10.1155/2013/692302>.
- [10] Y. Wang, W. Gao, X. Shi, J. Ding, W. Liu, H. He, K. Wang, F. Shao, Chemotherapy drugs induce pyroptosis through caspase-3 cleavage of a gasdermin, *Nature* 547 (2017) 99–103, <https://doi.org/10.1038/nature22393>.
- [11] B. Yuan, S. Pan, W.-W. Zhang, Effects of gangliosides on expressions of caspase-3 and NGF in rats with acute spinal cord injury, *Eur. Rev. Med. Pharmacol. Sci.* 21 (2017) 5843–5849, <https://doi.org/10.26355/eurev.201712.14033>.
- [12] Y.O. Mukhamedshina, E.R. Akhmetzyanova, E. V Martynova, S.F. Khaiboullina, L.R. Galieva, A.A. Rizvanov, Systemic and local cytokine profile following spinal cord injury in rats: a multiplex analysis, *Front. Neurol.* 8 (2017) 581, <https://doi.org/10.3389/fneur.2017.00581>.
- [13] C.D. Thompson, J.C. Zurko, B.F. Hanna, D.J. Hellenbrand, A. Hanna, The therapeutic role of interleukin-10 after spinal cord injury, *J. Neurotrauma* 30 (2013) 1311–1324, <https://doi.org/10.1089/neu.2012.2651>.
- [14] Z. Zhou, X. Peng, R. Insolera, D.J. Fink, M. Mata, IL-10 promotes neuronal survival following spinal cord injury, *Exp. Neurol.* 220 (2009) 183–190, <https://doi.org/10.1016/j.expneurol.2009.08.018>.
- [15] S. Cao, G. Hou, Y. Meng, Y. Chen, L. Xie, B. Shi, Network pharmacology and molecular docking-based investigation of potential targets of Astragalus membranaceus and angelica sinensis compound acting on spinal cord injury, *Dis. Markers* 2022 (2022) 2141882, <https://doi.org/10.1155/2022/2141882>.
- [16] N. Venkatasubramanian, C.F. Lee, S.H. Young, S.S. Tay, T. Umaphathi, A.Y. Lao, H.H. Gan, A.C. Baroque II, J.C. Navarro, H.M. Chang, J.M. Advincula, S. Muengtawepongsa, B.P.L. Chan, C.L. Chua, N. Wijekoon, H.A. de Silva, J.H.B. Hiyadan, N.C. Suwanwela, K.S.L. Wong, N. Pongvarin, G.B. Eow, C.L. H. Chen, C.-E.S. Investigators, Prognostic factors and pattern of long-term recovery with MLC601 (NeuroAid™) in the Chinese medicine NeuroAid efficacy on stroke recovery - extension study, *Cerebrovasc. Dis.* 43 (2017) 36–42, <https://doi.org/10.1159/000452285>.
- [17] H. Moha Ou Maati, M. Borsotto, F. Chatelain, C. Widmann, M. Lazdunski, C. Heurteaux, Activation of ATP-sensitive potassium channels as an element of the neuroprotective effects of the Traditional Chinese Medicine MLC901 against oxygen glucose deprivation, *Neuropharmacology* 63 (2012) 692–700, <https://doi.org/10.1016/j.neuropharm.2012.05.035>.
- [18] C. Heurteaux, C. Gandin, M. Borsotto, C. Widmann, F. Brau, M. Lhuillier, B. Onteniente, M. Lazdunski, Neuroprotective and neuroproliferative activities of NeuroAid (MLC601, MLC901), a Chinese medicine, in vitro and in vivo, *Neuropharmacology* 58 (2010) 987–1001, <https://doi.org/10.1016/j.neuropharm.2010.01.001>.
- [19] C. Heurteaux, C. Widmann, H. Moha ou Maati, H. Quintard, C. Gandin, M. Borsotto, J. Veyssiere, B. Onteniente, M. Lazdunski, NeuroAid: properties for neuroprotection and neurorepair, *Cerebrovasc. Dis.* 35 (2013) 1–7, <https://doi.org/10.1159/000346228>.
- [20] A. Al Fauzi, K.T. Prihastomo, I.G.M.A.R. Ranuh, T. Apriawan, J. Wahyuhadi, M.A. Parenrengi, A. Turchan, A.H. Bajamal, H.B. Notobroto, Clinical outcomes of MLC601 (NeuroAid(TM)) in traumatic brain injury: a pilot study, *Brain Sci.* 10 (2020) 60, <https://doi.org/10.3390/brainsci10020060>.
- [21] R. Kumar, O. Htwe, A. Baharudin, S.A. Rhani, K. Ibrahim, J.S. Nanra, M. Gsangaya, H. Harun, K. Kandar, M. Balan, S. Peh, Y. Pokharkar, A. Ingole, M. Hisam Ariffin, Spinal cord injury - assessing tolerability and use of combined rehabilitation and NeuroAid (SATURN) study - primary results of an exploratory study, *J. Spinal Cord Med.* 46 (2023) 682–686, <https://doi.org/10.1080/10790268.2022.2067972>.
- [22] Wahyudi, A.A. Islam, M. Hatta, W. Adhimarta, M. Faris, N. Mustamir, A. Bukhari, Prihantono, C. Kaelan, J. Hendarto, N.H. Imran, R.M. Rosyidi, The role of MLC901 in reducing VEGF as a vascular permeability marker in rats with spinal cord injury, *Ann. Med. Surg.* 75 (2022) 103344, <https://doi.org/10.1016/j.amsu.2022.103344>.
- [23] I.G.M.A.R. Ranuh, G.M. Sari, B. Utomo, N.S. Suroto, A. Al Fauzi, Systematic review and meta-analysis of the efficacy of MLC901 (NeuroAid II(TM)) for acute ischemic brain injury in animal models, *J. Evidence-based integr. Med.* 26 (2021), <https://doi.org/10.1177/2515690X211039219>, 2515690X211039219–2515690X211039219.
- [24] A.B. Nair, S. Jacob, A simple practice guide for dose conversion between animals and human, *J. Basic Clin. Pharm.* 7 (2016) 27–31, <https://doi.org/10.4103/0976-0105.177703>.
- [25] Instech, Guide to Oral Gavage for Mice and Rats, Instech Blog, 2020. <https://www.instechlabs.com/blog/guide-to-oral-gavage-for-mice-and-rats>. (Accessed 12 November 2023).
- [26] R. Verma, J.K. Virdi, N. Singh, A.S. Jaggi, Animals models of spinal cord contusion injury, *Korean J. Pain* 32 (2019) 12–21, <https://doi.org/10.3344/kjp.2019.32.1.12>.
- [27] Z. Hong, H. Hong, H. Chen, Z. Wang, D. Hong, Investigation of the protective effect of erythropoietin on spinal cord injury in rats, *Exp. Ther. Med.* 2 (2011) 837–841, <https://doi.org/10.3892/etm.2011.285>.
- [28] M. Liu, P. Bose, G.A. Walter, F.J. Thompson, K. Vandenborne, A longitudinal study of skeletal muscle following spinal cord injury and locomotor training, *Spinal Cord* 46 (2008) 488–493, <https://doi.org/10.1038/sj.sc.3102169>.
- [29] D.M. Basso, M.S. Beattie, J.C. Bresnahan, Graded histological and locomotor outcomes after spinal cord contusion using the NYU weight-drop device versus transection, *Exp. Neurol.* 139 (1996) 244–256, <https://doi.org/10.1006/exnr.1996.0098>.
- [30] W. Huang, X. Bai, E. Meyer, A. Scheller, Acute brain injuries trigger microglia as an additional source of the proteoglycan NG2, *Acta Neuropathol., Commun.* Now. 8 (2020) 146, <https://doi.org/10.1186/s40478-020-01016-2>.
- [31] A.R. Hackett, J.K. Lee, Understanding the NG2 glial scar after spinal cord injury, *Front. Neurol.* 7 (2016) 199, <https://doi.org/10.3389/fneur.2016.00199>.
- [32] A.P. Tran, P.M. Warren, J. Silver, The biology of regeneration failure and success after spinal cord injury, *Physiol. Rev.* 98 (2018) 881–917, <https://doi.org/10.1152/physrev.00017.2017>.

- [33] K. Tansey, B.A. Kakulas, Criteria for biological interventions for spinal cord injury repair, *Restor. Neurol. Spinal Cord Inj* (2011) 169–180, <https://doi.org/10.1093/acprof:oso/9780199746507.003.0007>.
- [34] A. Sharma, B.L. Fish, J.E. Moulder, M. Medhora, J.E. Baker, M. Mader, E.P. Cohen, Safety and blood sample volume and quality of a refined retro-orbital bleeding technique in rats using a lateral approach, *Lab Anim. (NY)*. 43 (2014) 63–66, <https://doi.org/10.1038/labani.432>.
- [35] D.P.W. Wardhana, A.B.S. Satyarsa, R.M. Rosyid, H. Harmansyah, T.G.B. Mahadewa, A.A. Islam, I.M. Jawi, S. Maliawan, The potential of MLC901 as adjuvant therapy for traumatic spinal cord injury by multi-pathway biomechanism: a systematic review, *Bali Med. J.* 12 (2023) 2130–2141, <https://doi.org/10.15562/bmj.v12i2.4606>.
- [36] V. Rakkhitawattana, C. Sillapachaiyaporn, S. Nilkhet, J. Brimson, T. Tencomnao, Effect of Thai medicinal plants *Acanthus ebracteatus* Vahl. *Carthamus tinctorius* L. and *Streblus asper* Lour. on neurite outgrowth activity in Neuro-2A cells, *J. Assoc. Med. Sci.* 56 (2023) 71–84, <https://doi.org/10.12982/jams.2023.010>.
- [37] Y. Lu, J. Yang, X. Wang, Z. Ma, S. Li, Z. Liu, X. Fan, Research progress in use of traditional Chinese medicine for treatment of spinal cord injury, *Biomed. Pharmacother.* 127 (2020) 110136, <https://doi.org/10.1016/j.biopha.2020.110136>.
- [38] Q. Zhang, H. Yang, J. An, R. Zhang, B. Chen, D.-J. Hao, Therapeutic effects of traditional Chinese medicine on spinal cord injury: a promising supplementary treatment in future, *evid. Based. Complement. Alternat. Med.* 2016 (2016) 8958721, <https://doi.org/10.1155/2016/8958721>.
- [39] Z. Huang, J. Wang, C. Li, W. Zheng, J. He, Z. Wu, J. Tang, Application of natural antioxidants from traditional Chinese medicine in the treatment of spinal cord injury, *Front. Pharmacol.* 13 (2022) 976757, <https://doi.org/10.3389/fphar.2022.976757>.
- [40] X. Chen, Y. Wang, Y. Ma, R. Wang, D. Zhao, To explore the *Radix Paeoniae Rubra-Flos Carthami* herb pair's potential mechanism in the treatment of ischemic stroke by network pharmacology and molecular docking technology, *Medicine (Baltim.)* 100 (2021) e27752, <https://doi.org/10.1097/MD.00000000000027752>.
- [41] C. Widmann, C. Gandin, A. Petit-Paitel, M. Lazdunski, C. Heurteaux, The Traditional Chinese Medicine MLC901 inhibits inflammation processes after focal cerebral ischemia, *Sci. Rep.* 8 (2018) 18062, <https://doi.org/10.1038/s41598-018-36138-0>.
- [42] B. Tao, Q. Wang, J. Cao, Y. Yasen, L. Ma, C. Sun, J. Shang, S. Feng, The mechanisms of *Chuanxiong Rhizoma* in treating spinal cord injury based on network pharmacology and experimental verification, *Ann. Transl. Med.* 9 (2021) 1145, <https://doi.org/10.21037/atm-21-2529>.
- [43] I. Aziz, M.D. Che Ramli, N.S. Mohd Zain, J. Sanusi, Behavioral and histopathological study of changes in spinal cord injured rats supplemented with spirulina platensis, *evid. Based. Complement. Alternat. Med.* 2014 (2014) 871657, <https://doi.org/10.1155/2014/871657>.
- [44] R. Keikhaei, E. Abdi, M. Darvishi, Z. Ghotbeddin, H.G. Hamidabadi, Combined treatment of high-intensity interval training with neural stem cell generation on contusive model of spinal cord injury in rats, *Brain Behav* 13 (2023) e3043, <https://doi.org/10.1002/brb3.3043>, e3043.
- [45] Z. Guo, R. Peng, J. Song, Potential mechanism of *Astragalus radix-Angelicae sinensis radix* in the treatment of spinal cord injury based on network pharmacology and molecular docking, *TMR Pharmacol. Res.* 1 (2021) 7, <https://doi.org/10.53388/tmpr20210402007>.
- [46] L. Zhou, Z. Song, L. Zhou, Y. Qiu, N. Hu, Y. Hu, X. Hu, Protective role of astragalus injection in spinal cord ischemia-reperfusion injury in rats, *Neurosciences* 23 (2018) 116–121, <https://doi.org/10.17712/nsj.2018.4.20170391>.
- [47] J. Zhong, J. Zhou, H. Sun, Y. Wu, Y. Wu, M. Li, Effects of *Salvia miltiorrhiza* injection on apoptosis of Schwann cells induced by hydrogen peroxide, *Ann. Palliat. Med.* 10 (2021) 625–632, <https://doi.org/10.21037/apm-20-2580>.
- [48] J.-H. Kim, J.-W. Song, H. Joo, J.-W. Park, B. Lee, J.-H. Cho, K. Lee, H. Lee, J. Park, J.-W. Jeong, E.-J. Kim, Y. Bu, A review on the pharmacological activities of *salvia miltiorrhiza* radix using international classification of disease, 10th Revision (ICD-10) codes, *Processes* 10 (2022) 1860, <https://doi.org/10.3390/pr10091860>.
- [49] F. Jiao, K. Varghese, S. Wang, Y. Liu, H. Yu, G.W. Booz, R.J. Roman, R. Liu, F. Fan, Recent insights into the protective mechanisms of paeoniflorin in neurological, cardiovascular, and renal diseases, *J. Cardiovasc. Pharmacol.* 77 (2021) 728–734, <https://doi.org/10.1097/FJC.0000000000001021>.
- [50] Y. Xie, H. Zhang, Y. Zhang, C. Wang, D. Duan, Z. Wang, Chinese angelica polysaccharide (CAP) alleviates LPS-induced inflammation and apoptosis by down-regulating COX-1 in PC12 cells, *Cell. Physiol. Biochem.* 49 (2018) 1380–1388, <https://doi.org/10.1159/000493415>.
- [51] L. Wang, B.O.A. Botchway, X. Liu, The repression of the HMGB1-TLR4-NF- $\kappa$ B signaling pathway by safflower yellow may improve spinal cord injury, *Front. Neurosci.* 15 (2021) 803885, <https://doi.org/10.3389/fnins.2021.803885>.
- [52] Z. Lin, J. Gu, J. Xiu, T. Mi, J. Dong, J.K. Tiwari, Traditional Chinese medicine for senile dementia, *Evid. Based. Complement. Alternat. Med.* 2012 (2012) 692621, <https://doi.org/10.1155/2012/692621>.
- [53] T. Kuboyama, K. Hirotsu, T. Arai, H. Yamasaki, C. Tohda, *Polygalae radix* Extract prevents axonal degeneration and memory deficits in a transgenic mouse model of Alzheimer's disease, *Front. Pharmacol.* 8 (2017) 805, <https://doi.org/10.3389/fphar.2017.00805>.